Am J Physiol Cell Physiol 289: C68–C81, 2005.
First published February 23, 2005; doi:10.1152/ajpcell.00631.2004.

Is myosin light-chain phosphorylation a regulatory signal for the osmotic activation of the Na^+-K^+-$2Cl^-$ cotransporter?

Caterina Di Ciano-Oliveira,[1] Monika Lodyga,[1] Lingzhi Fan,[1] Katalin Szászi,[1] Hiroshi Hosoya,[2] Ori D. Rotstein,[1] and András Kapus[1]

[1]*Department of Surgery, The Toronto General Hospital and University Health Network, Toronto, Ontario, Canada; and* [2]*Department of Biological Science, Graduate School of Science, Hiroshima University, Higashi-Hiroshima, Japan*

Submitted 22 December 2004; accepted in final form 16 February 2005

Di Ciano-Oliveira, Caterina, Monika Lodyga, Lingzhi Fan, Katalin Szászi, Hiroshi Hosoya, Ori D. Rotstein, and András Kapus. Is myosin light-chain phosphorylation a regulatory signal for the osmotic activation of the Na^+-K^+-$2Cl^-$ cotransporter? *Am J Physiol Cell Physiol* 289: C68–C81, 2005. First published February 23, 2005; doi:10.1152/ajpcell.00631.2004.—Myosin light-chain (MLC) kinase (MLCK)-dependent increase in MLC phosphorylation has been proposed to be a key mediator of the hyperosmotic activation of the Na^+-K^+-$2Cl^-$ cotransporter (NKCC). To address this hypothesis and to assess whether MLC phosphorylation plays a signaling or permissive role in NKCC regulation, we used pharmacological and genetic means to manipulate MLCK, MLC phosphorylation, or myosin ATPase activity and followed the impact of these alterations on the hypertonic stimulation of NKCC in porcine kidney tubular LLC-PK1 epithelial cells. We found that the MLCK inhibitor ML-7 suppressed NKCC activity independently of MLC phosphorylation. Notably, ML-7 reduced both basal and hypertonically stimulated NKCC activity without influencing MLC phosphorylation under these conditions, and it inhibited NKCC activation by Cl^- depletion, a treatment that did not increase MLC phosphorylation. Furthermore, prevention of the osmotically induced increase in MLC phosphorylation by viral induction of cells with a nonphosphorylatable, dominant negative MLC mutant (AA-MLC) did not affect the hypertonic activation of NKCC. Conversely, a constitutively active MLC mutant (DD-MLC) that mimics the diphosphorylated form neither stimulated isotonic nor potentiated hypertonic NKCC activity. Furthermore, a depolarization-induced increase in endogenous MLC phosphorylation failed to activate NKCC. However, complete abolition of basal MLC phosphorylation by K252a or the inhibition of myosin ATPase by blebbistatin significantly reduced the osmotic stimulation of NKCC without suppressing its basal or Cl^- depletion-triggered activity. These results indicate that an increase in MLC phosphorylation is neither a sufficient nor a necessary signal to stimulate NKCC in tubular cells. However, basal myosin activity plays a permissive role in the optimal osmotic responsiveness of NKCC.

proline-alanine-rich STE20-related kinase

THE NA^+-K^+-$2CL^-$ COTRANSPORTER (NKCC) is a loop diuretic-sensitive electroneutral ion translocator that plays vital roles in salt and water secretion and reabsorbtion, thereby regulating the fluid homeostasis of the whole organism. NKCC is also a key component of volume regulation at the single-cell level as a major mediator of regulatory volume increase, an adaptive response to cell shrinkage (16, 17, 48). The NKCC family consists of two isoforms: the ubiquitously expressed NKCC1, which in secretory epithelial cells is localized to the basolateral membrane, and NKCC2, the apical or reabsorptive isoform, which is expressed in cells of the macula densa and the thick ascending limb of Henle in the kidney (17, 19). There are two main physiological parameters that regulate both isoforms: intracellular Cl^- concentration ($[Cl^-]_i$) and cell volume (4, 22, 37, 38, 47). A decrease in $[Cl^-]_i$ or in cell volume induces the phosphorylation of NKCC on threonine (and potentially on serine) residues and concomitantly leads to the activation of the cotransporter (7, 18, 38, 43). Recently, the proline-alanine-rich STE20-related kinase (PASK) has emerged as an attractive candidate for mediation of NKCC phosphorylation, because it binds to NKCC (10, 46), it can be activated by both Cl^- depletion and cell shrinkage, and its dominant negative form inhibits NKCC activation by these stimuli (10). However, disruption of the PASK-NKCC binding did not affect NKCC activation (45). Thus, while the identity of the responsible kinases remains an intriguing question, it appears plausible that PASK and/or an as yet unidentified PASK-like kinase participate in NKCC phosphorylation and regulation.

Interestingly, cell shrinkage is thought to activate NKCC through another mechanism as well, which presumably is independent of its direct phosphorylation but involves the phosphorylation of the myosin light chain (MLC) and the ensuing increase in cell contractility (26). This notion is based on observations that cell shrinkage provoked the phosphorylation of MLC (26, 53) on Thr18 and Ser19 (9) and pharmacological inhibition of MLC phosphorylation by MLC kinase (MLCK) inhibitors prevented or reduced the hyperosmotic (9, 26, 27) or agonist-induced (1, 20) stimulation of NKCC. However, other findings cast doubt on the validity of this conclusion as inferred from the above inhibitor experiments, the vast majority of which were based on the use of ML-7, or the related ML-9, piperazine-derivative inhibitors of MLCK. Remarkably, while in certain cell types ML-7 potently inhibited the shrinkage-induced activation of NKCC (with $K_i < 0.5$ μM corresponding to its effect on MLCK) (27, 43), the required inhibitor concentration was two orders of magnitude higher in other cells (9, 26), in which the drug may not be sufficiently specific and could affect NKCC activation independently of MLCK (3, 25, 49). Accordingly, it remained to be tested whether ML-7 selectively abrogates the hypertonic regulation of NKCC or also interferes with the contractility-independent (e.g., Cl^- depletion induced) activation of the cotransporter. Moreover, our previous studies (9) showed that in LLC-PK1 porcine kidney tubular cells, the majority of the osmotically induced MLC phosphorylation is mediated by the

Address for reprint requests and other correspondence: A. Kapus, St. Michael's Hospital, Research Institute, Queen Wing 7009, 30 Bond St., Toronto, ON, Canada M5B 1W8 (e-mail: kapusa@smh.toronto.on.ca).

The costs of publication of this article were defrayed in part by the payment of page charges. The article must therefore be hereby marked "*advertisement*" in accordance with 18 U.S.C. Section 1734 solely to indicate this fact.

0363-6143/05 $8.00 Copyright © 2005 the American Physiological Society

Downloaded from journals.physiology.org/journal/ajpcell (106.051.226.007) on August 4, 2022.

Rho-Rho kinase (ROK) pathway. While the inhibition of ROK drastically reduced hypertonicity-provoked MLC phosphorylation, it had no effect on hypertonic NKCC stimulation. In contrast, ML-7 efficiently reduced osmotic NKCC activation but only marginally affected MLC phosphorylation. The substantial uncoupling between the two phenomena raised the question whether a cause-and-effect relationship exists between MLC phosphorylation and NKCC activation or whether these phenomena are parallel but independent events. Even if such a relationship exists, however, it remains to be determined whether an increase in myosin phosphorylation is in fact a signal for the osmotic activation of NKCC or whether a basal level of MLC phosphorylation (or myosin ATPase activity) is merely a permissive factor necessary for the maximal osmotic stimulation of the cotransporter. Finally, MLCK-mediated regulation does not necessarily occur through myosin phosphorylation, because MLCK can activate myosin ATPase activity without phosphorylation (14, 54), and MLCK has been reported to act on transporters in a myosin-independent manner (50).

To address the above-described possibilities, we tested the effect of ML-7 on the osmotically stimulated and Cl^- depletion-triggered activation of NKCC and compared the effect of ML-7 with a structurally different MLCK inhibitor. Besides this pharmacological approach, we applied genetic tools as well. We generated retroviruses expressing MLC mutants that mimic either the nonphosphorylated or the doubly phosphorylated forms of MLC (13, 24) and showed that they act as dominant negative and constitutively active variants, respectively. We then determined the effect of these MLC mutants on endogenous MLC phosphorylation and NKCC activity. Finally, to discriminate the role of myosin phosphorylation per se from myosin ATPase activity, we used blebbistatin, a novel and highly specific myosin II ATPase inhibitor. Our results show that in LLC-PK1 cells, ML-7 inhibits NKCC, but not via the inhibition of MLCK. Furthermore, a rise in MLC phosphorylation is not a signal to activate NKCC, because it is neither necessary nor sufficient for the full osmotic stimulation of the transporter. On the other hand, basal myosin ATPase activity is a prerequisite for the complete osmotic activation of NKCC, suggesting that it exerts a permissive effect.

MATERIALS AND METHODS

Chemicals and antibodies. Bumetanide, ouabain, polybrene, and TGF-β_1 were obtained from Sigma (St. Louis, MO). Blebbistatin, ML-7, latrunculin B (LatB), and Y-27632 were purchased from Calbiochem (San Diego, CA). Toxin B isolated from *Clostridium difficile* was purchased from TechLab (Blacksburg, VA), and K252a was obtained from Biomol (Plymouth Meeting, PA). Rhodamine-labeled phalloidin was purchased from Molecular Probes (Eugene, OR). *Eco*RI, *Xho*I, *Taq*, and *Pfu* were obtained from New England BioLabs (Beverly, MA), and DNA ligase was purchased from GIBCO-BRL (Grand Island, NY). The following antibodies were used. Monoclonal anti-Myc, polyclonal anti-MLC, and peroxidase-conjugated anti-goat antibodies were obtained from Santa Cruz Biotechnology (Santa Cruz, CA). Polyclonal antibody directed against diphosphorylated MLC (i.e., phospho-Thr18 and phospho-Ser19) were purchased from Cell Signaling Technology (Beverly, MA) and Santa Cruz Biotechnology. Anti-rabbit fluorescein isothiocyanate (FITC), anti-goat FITC, and anti-mouse Cy3 were obtained from Jackson ImmunoResearch (West Grove, PA). Peroxidase-conjugated anti-mouse antibody was purchased from Amersham (Piscataway, NJ).

Cell culture. The porcine kidney epithelial cell line, LLC-PK1, was used for all experiments. This cell line offers two major advantages relevant to the investigated question. Hypertonicity induces sizable and well-quantifiable MLC phosphorylation in LLC-PK1 cells, and the basic characteristics of this process have been described in our previous studies (9). LLC-PK1 cells possess substantial NKCC activity under basal conditions that is activated severalfold upon hypertonic exposure. For the generation of viral particles, AAV-293 cells (Stratagene, La Jolla, CA) were used. Cells were grown in a humidified atmosphere of air-CO_2 (19:1 vol/vol) at 37°C in Dulbecco's modified Eagle's medium (DMEM; GIBCO-BRL) supplemented with 10% fetal bovine serum (Sigma) and 1% antibiotic suspension (penicillin and streptomycin; Sigma).

Media and cell treatment. For serum depletion, cells were incubated in HCO_3^--free RPMI 1640 buffered with 25 mM HEPES to pH 7.4 (HPMI; osmolarity 290 ± 5) for 3 h. The following media were used for treatments. The isotonic NaCl medium (Iso NaCl) consisted of (in mM) 130 NaCl, 3 KCl, 1 $MgCl_2$, 1 $CaCl_2$, 20 HEPES, pH 7.4, and 5 glucose. An isotonic sodium methane sulfonic acid (Iso NaMSA)-based solution was used for Cl^- depletion and consisted of (in mM) 125 methane sulfonic acid, 125 NaOH, 3 KOH, 1 $MgSO_4$, 1 $CaSO_4$, 20 HEPES, pH 7.4, and 5 glucose. To achieve membrane depolarization, we used an isotonic KCl (Iso KCl) medium containing (in mM) 130 KCl, 3 NaCl, 1 $MgCl_2$, 1 $CaCl_2$, 20 HEPES, and 5 glucose. Cell-cell contact disassembly was induced by replacing 1 mM $CaCl_2$ with 1 mM EGTA in the Iso NaCl and Iso KCl solutions. For ^{86}Rb uptake experiments, Iso NaCl and Iso NaMSA were supplemented with 2 mM KCl or KOH, respectively (final concentration 5 mM), and 0.3 mM Na_2HPO_4. Hyperosmolarity was achieved by the addition of either 100 mM sucrose for the ^{86}Rb uptake assays or 300 mM sucrose for all other experiments. Unless otherwise stated, LLC-PK1 cells were grown to confluence, serum deprived in HPMI for 3 h, and then preincubated with Iso NaCl solution for 10–30 min. They were then treated as described in the figure legends.

Plasmids. Plasmids encoding green fluorescent protein (GFP; Clontech, Palo Alto, CA) and C3 transferase, an enzyme that inactivates Rho via ADP ribosylation (2), were described previously. Wild-type myosin regulatory light chain MRLC2 (WT-MLC) or mutant MRLC2 in which Thr18 and Ser19 were replaced with alanines (AA-MLC) or with aspartic acid (DD-MLC) were cloned into pcDNA3.1 with COOH-terminal Myc and His tags as described previously (24). For viral transduction, we subcloned WT-, AA-, and DD-MLC into the retroviral expression vector, pFB-Neo (Stratagene) as follows. The inserts were amplified from the pcDNA3.1 using primers 5′-CGGAATTCCGCCACCATGTCGAGCAAAAAG-3′ (forward) and 5′-CGCTCGAGTCAATGGTGATGGTGATG-3′ (reverse) so that the COOH-terminal Myc and His tags were maintained. The purified PCR products (WT-, AA-, and DD-MLC) were then cloned into the pFB-Neo at the *Eco*RI and *Xho*I restriction sites. The presence of an insert was verified by digestion with *Eco*RI and *Xho*I. Subsequently, the mutants were verified by performing sequence analysis.

Transient transfection. Transient transfection was performed using FuGene6 reagent (Roche, Indianapolis, IN) according to the manufacturer's instructions. Unless otherwise stated, cells were transfected with 1 μg of plasmid DNA per well of a six-well plate. The DNA-to-FuGene6 reagent ratio was 1 μg to 2.5 μl, respectively. The details of cotransfection are specified under the corresponding figures.

Preparation of viral particles and viral transduction of LLC-PK1 cells. The pVPack system from Stratagene was used to prepare viral particles from pFB-Neo vectors containing the WT-, AA-, and DD-MLC inserts. Briefly, AAV-293 cells growing in T75 tissue culture flasks were triple transfected at 30% confluence with 4 μg each of pVPack-GP gag-pol-expressing vector, pVPack-VSV-G envelope-expressing vector, and pFB-Neo (WT-, AA-, or DD-MLC) using FuGene6 transfection reagent. After 12–16 h, the growth medium (i.e., DMEM with serum and antibiotics) was replaced with 9 ml of fresh growth medium. After an additional 72 h, the medium was

Downloaded from journals.physiology.org/journal/ajpcell (106.051.226.007) on August 4, 2022.

collected and centrifuged at 2,000 rpm for 10 min. The supernatants containing viral particles were then filtered with 0.45-μm Millex HV filters (Millipore, Billerica, MA) and stored in working aliquots at −80°C until further use. LLC-PK1 cells were transduced as follows. Supernatants containing viral particles were mixed with growth medium (2:1 vol/vol for 6-well plates or 3:1 vol/vol for 12-well plates) and supplemented with 25 μM polybrene (Sigma). This mixture was applied to LLC-PK1 cells at 30% confluence for 16 h and subsequently was replaced with normal growth medium. After an additional 48 h, experiments were performed.

Determination of NKCC activity. NKCC activity was monitored by analyzing the bumetanide-sensitive cellular uptake of ^{86}Rb essentially as described previously (9). Briefly, confluent LLC-PK1 cells grown in 12-well plates were serum depleted for 3 h. Cells were then incubated in Iso NaCl for 10 min, followed by pretreatment with Iso NaCl (for subsequent isotonic and hypertonic treatment) or with Iso MSA (for Cl^- depletion) for another 30 min. The Na^+-K^+ pump inhibitor ouabain (1 mM) was then added for 2 min. Finally, cells were treated with Iso NaCl (for isotonic and Cl^- depletion experiments) or Iso NaCl + 100 mM sucrose (for hypertonic experiments) containing 1 mM ouabain and 1.5 μCi ^{86}Rb. After 7 min (or as indicated for the time course), the cells were washed 5 times with ice-cold 0.1 M $MgCl_2$, air dried, and dissolved in 0.2% SDS. The amount of ^{86}Rb taken up by the cells was measured using an LS-6500 scintillation counter (Beckman Coulter, Fullerton, CA). When present, pharmacological inhibitors were added to all solutions at the same concentration. To determine the NKCC-dependent component of ^{86}Rb uptake, all experiments were performed in the presence or absence of bumetanide (100 μM), which was added at the same time as ouabain.

Statistical analysis. ^{86}Rb uptake experiments were performed three times, and if not specified otherwise (see dose-response curve shown in Fig. 1*C*), duplicate or triplicate experiments were performed for each condition. The NKCC activity (expressed as nmol K^+/7 min/well) was calculated after subtracting the bumetanide-insensitive fraction. The protein content per well was 227 ± 6 μg (n = 24 wells) as determined using random sampling. Protein determination and visual inspection showed that none of the treatments caused detachment of cells from the wells. One-way ANOVA or unpaired t-tests (see Fig. 6*C*) were performed using GraphPad Prism version 4.00 software (GraphPad Software, San Diego, CA). $P < 0.05$ was considered statistically significant.

Determination of MLC phosphorylation using urea glycerol PAGE.

SAMPLE PREPARATION. After treatment, LLC-PK1 cells grown in six-well plates were lysed in 950 μl of ice-cold acetone containing 10% trichloroacetic acid and 10 mM dithiothreitol. The cell lysates were then scraped from the wells and centrifuged for 10 min at 12,000 rpm. The resulting pellet was washed with 1 ml of pure acetone, allowed to air dry, and dissolved for 1 h in 60 μl of freshly made sample buffer containing 8.02 M urea, 234 mM sucrose, 23 mM glycine, 10.4 mM dithiothreitol, 20 mM Tris-Base, pH 8.6, and 0.01% bromophenol blue. Samples were then centrifuged for 10 min at 12,000 rpm, and 40–45 μl of supernatant were loaded onto the urea glycerol gels as described previously (9).

ELECTROPHORESIS. Twelve percent urea glycerol gels were prerun for 1 h at 180 V in running buffer containing 23 mM glycine, 20 mM Tris-Base, pH 8.6, 2.44 mM thioglycolic acid, and 0.97 mM dithiothreitol. Samples were then loaded, and the gels were run at 260 V for 1 h and at 300 V for ~2.5 h. The gels were then transferred to nitrocellulose using a mini-electrophoretic transfer cell (Bio-Rad Laboratories, Hercules, CA). Blots were blocked in Tris-buffered saline (TBS) containing 5% bovine serum albumin (Sigma) and incubated with the corresponding primary antibody. Binding of the antibody was visualized using the relevant (anti-mouse or anti-goat) peroxidase-conjugated secondary antibodies (1:3,000 dilution) with enhanced chemiluminescence (PerkinElmer, Boston, MA). Densitometric analysis of blots was performed using a Bio-Rad GS-690 imaging densitometer and Molecular Analyst software (version 1.5; Bio-Rad Laboratories) as described previously (9).

Immunofluorescence. After treatment, confluent cells grown on 25-mm coverslips were fixed for 30 min in the treatment medium supplemented with 4% paraformaldehyde. The coverslips were extensively washed with PBS, incubated with 100 mM glycine in PBS for 10 min, permeabilized with 0.1% Triton X-100 in PBS for 20 min, and then blocked in 5% bovine serum albumin in TBS for 1 h. Subsequently, the samples were incubated with primary antibodies for 1 h, washed with PBS, and incubated with fluorescently labeled secondary antibody for 1 h. The coverslips were then washed and mounted on glass slides using Dako mounting solution. The staining was visualized using a Nikon Eclipse TE200 fluorescent microscope (×100 and ×20 lens objectives) coupled to a cooled, charge-coupled device camera (C4742-95; Hamamatsu Photonics, Hamamatsu City, Japan) driven by Simple PCI software.

RT-PCR for NKCC1 and NKCC2. Total RNA was extracted from LLC-PK1 cells, porcine aortic endothelial cells (PAECs), mouse embryonic fibroblasts (MEFs), and whole kidney of Black 6 mice using TRIzol (Invitrogen, San Diego, CA) according to the manufacturer's instructions. cDNA was synthesized from 5 μg of total RNA using SuperScript II Reverse Transcriptase (Invitrogen) and poly(A)$^+$·oligo(dT)$_{12–18}$ as a template primer. The cDNA were subsequently subjected to PCR using specific primers for NKCC1, NKCC2, and β-actin. The specific primers were designed from the alignment of human, mouse, and rat sequences for NKCC1 and NKCC2 and pig, mouse, and human sequences for β-actin. The primers were as follows. For NKCC1, the forward primer was 5′-CGGAGAGCGATGGCTACTTT-3′ and the reverse primer was 5′-CAGAAGGCACCTCAAGGCTAA-3′ with an estimated 800-bp amplicon. For NKCC2, the forward primer was 5′-CAGCTTTAGGCCTGGGAATCA-3′ and the reverse primer was 5′-GCCTATTGACCCACCGAACTC-3′ with an estimated 600-bp amplicon. For β-actin, the forward primer was 5′-AACTGGGACGACATGGAGAA-3′ and the reverse primer was 5′-TACTCCTGCTTGCTGATCCAC-3′ with an estimated 700-bp amplicon. Each reaction was performed with 2 μl of cDNA from the RT-PCR reaction, 0.3 μl of 10× PCR buffer, 1 μl of 50 mM $MgCl_2$, 0.7 μl of 10 mM dNTP, 1 μl each of forward and reverse primers, 0.3 μl of *Taq* DNA polymerase (5 U/μl), and 21 μl of sterile distilled water. The PCR products were separated on 0.8% agarose gel.

RESULTS

Effect of ML-7 on basal, hypertonicity-stimulated, and Cl^- depletion-induced activity of NKCC in kidney tubular cells. Initially, we characterized the time dependence of NKCC activity under isotonic and hypertonic conditions in porcine kidney tubular LLC-PK1 cells by measuring the ouabain-insensitive and bumetanide-sensitive uptake of ^{86}Rb during a period of 15 min. Figure 1*A* shows that under isotonic conditions, ^{86}Rb uptake increased linearly in this time range. When hypertonic stress was induced by 100 mM sucrose concomitant with the addition of ^{86}Rb, there was no increase in the isotope uptake after 1 min; however, after 3 min, ^{86}Rb uptake increased linearly and its rate was 3.6-fold that under isotonic conditions (Fig. 1*A*). The initial lag phase likely corresponds to the time required for the activation of NKCC as reported previously (36, 44). On the basis of these observations, we measured ^{86}Rb uptake at 7 min for all subsequent experiments, when isotope accumulation was strictly linear with time and sufficient to provide good resolution for inhibitor studies. Figure 1*B* shows that under isotonic conditions, the bumetanide-sensitive uptake was ~60% of the total ouabain-insen-

Downloaded from journals.physiology.org/journal/ajpcell (106.051.226.007) on August 4, 2022.

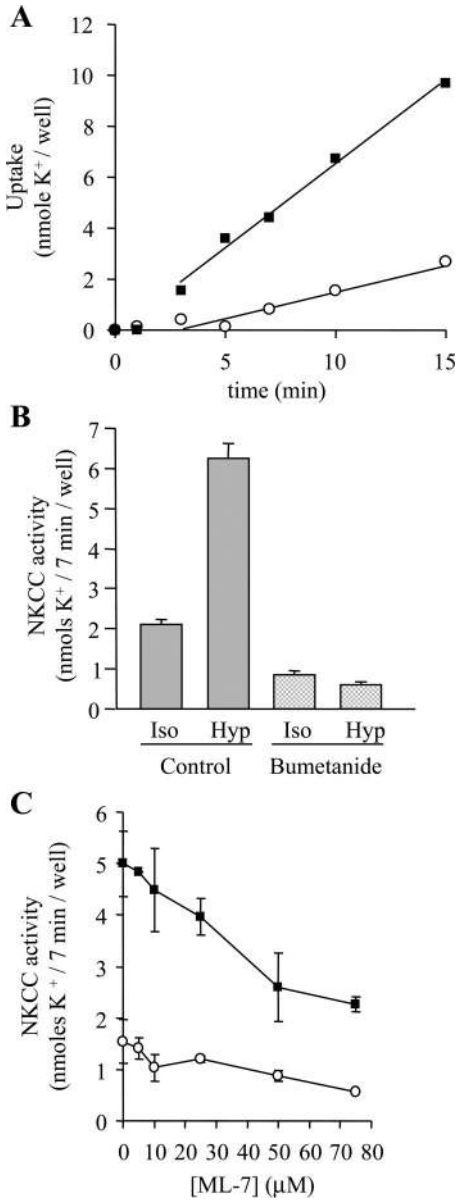

Fig. 1. Time dependence and ML-7 sensitivity of Na^+-K^+-$2Cl^-$ cotransporter (NKCC) activity under isotonic (Iso, ○) and hypertonic (Hyp, ■) conditions in LLC-PK1 cells. Confluent LLC-PK1 cells were serum deprived for 3 h and then preincubated with isotonic NaCl medium (Iso NaCl) for 10 min. Unless otherwise stated, this pretreatment was performed for all subsequent experiments. NKCC activity was then measured as the bumetanide-sensitive (and ouabain-insensitive) uptake of ^{86}Rb (see MATERIALS AND METHODS). *A*: time course for hyperosmotic NKCC activation. LLC-PK1 cells were treated either isotonically or hypertonically with the addition of 100 mM sucrose to the Iso NaCl medium in the presence of 1.5 μCi ^{86}Rb for the indicated times. Two independent experiments were performed in duplicate for each time point. A representative experiment is shown. *B*: total and bumetanide-insensitive ^{86}Rb uptake. Ouabain-treated LLC-PK1 cells were challenged iso- or hypertonically in the presence or absence of bumetanide for 7 min as above ($n = 11$, with each experiment performed in duplicate or in triplicate). *C*: dose-dependent inhibition of NKCC activity by ML-7. Serum-deprived LLC-PK1 cells were preincubated in Iso NaCl for 30 min in the absence or presence of various concentrations of ML-7. Cells were then treated isotonically or hypertonically for 7 min under the same inhibitor conditions, and ^{86}Rb uptake was determined ($n = 3$). For all subsequent experiments, cellular uptake of ^{86}Rb was measured after 7 min of treatment.

sitive uptake. Thus any measured change in isotope uptake reflected proportional changes in NKCC activity.

Previous studies (26, 27, 43), including our own (9), have indicated that the MLCK inhibitor ML-7 can substantially reduce hyperosmotic activation of NKCC. However, the sensitivity to ML-7 varied significantly in different cell types. To determine the ML-7 sensitivity of NKCC in LLC-PK1 cells, we investigated the dependence of the transport rate on ML-7 concentration. Fifty percent reduction in the hypertonically stimulated uptake rate was attained at ~50 μM ML-7, while 75 μM (the routinely applied maximal concentration) caused ~60% inhibition (Fig. 1*C*). No significant further inhibition was observed at 100 μM (data not shown), and to avoid potential toxic effects, higher concentrations were not applied. Interestingly, these studies indicated that the basal (i.e., isotonic) NKCC activity was also sensitive to ML-7. In fact, the drug inhibited the isotonic and hypertonically stimulated transport to the same extent, causing ~60% reduction at 75 μM (Fig. 1*C*). Furthermore, although the maximal hypertonic transport rates were strongly suppressed in the presence of ML-7, NKCC remained clearly activatable by osmotic stress, without any significant change in the relative increase over isotonic values. These observations suggested that ML-7 might not specifically target the osmotically induced signaling pathways responsible for NKCC stimulation. To substantiate this notion, we used Cl^- depletion, an alternative means by which to activate NKCC, and compared the effect of ML-7 on NKCC activity enhanced by Cl^- depletion, hypertonicity, or the combination of these stimuli. Cl^- depletion was achieved by incubating LLC-PK1 cells in an isotonic Cl^--free, methane sulfonic acid-based solution (Iso NaMSA) for 30 min (38), followed by readdition of Cl^- under iso- or hypertonic conditions in the presence of ^{86}Rb. As shown in Fig. 2*A*, compared with the isotonic control, NKCC activity was increased 4.0- and 4.2-fold by Cl^- depletion and hyperosmotic stress, respectively. Importantly, the effect of the two stimuli together was only slightly higher than it was after stimulation with these entities individually, suggesting either that each of the triggering factors can exert a near-maximal effect individually or that they use largely overlapping signaling mechanisms (Fig. 2*A*). Next, we determined the effect of ML-7 under these same conditions. In the presence of 75 μM ML-7, NKCC activity was reduced by ~60% when stimulated by either Cl^- depletion or hyperosmolarity, or both, clearly indicating that this drug is not specific for hyperosmotic induced NKCC activation (Fig. 2*A*).

Because ML-7 suppressed the Cl^- depletion-induced NKCC activation, we wanted to determine whether Cl^- depletion resulted in increased MLC phosphorylation. To answer this question, LLC-PK1 cells were treated with either isotonic Cl^--containing or Cl^--free medium for 20 min or exposed to hypertonicity as a positive control. Subsequently, the differentially phosphorylated forms of MLC were separated using urea glycerol PAGE. In agreement with our previous findings (9), LLC-PK1 cells expressed two isoforms of MLC, both of which can be mono- or diphosphorylated. Accordingly, upon urea glycerol PAGE, MLC can be separated into three doublets (6 bands), with the two uppermost bands corresponding to nonphosphorylated MLC, the middle two bands corresponding to monophosphorylated MLC (pMLC), and the lower two bands corresponding to diphosphorylated MLC (ppMLC). Hyperos-

Downloaded from journals.physiology.org/journal/ajpcell (106.051.226.007) on August 4, 2022.

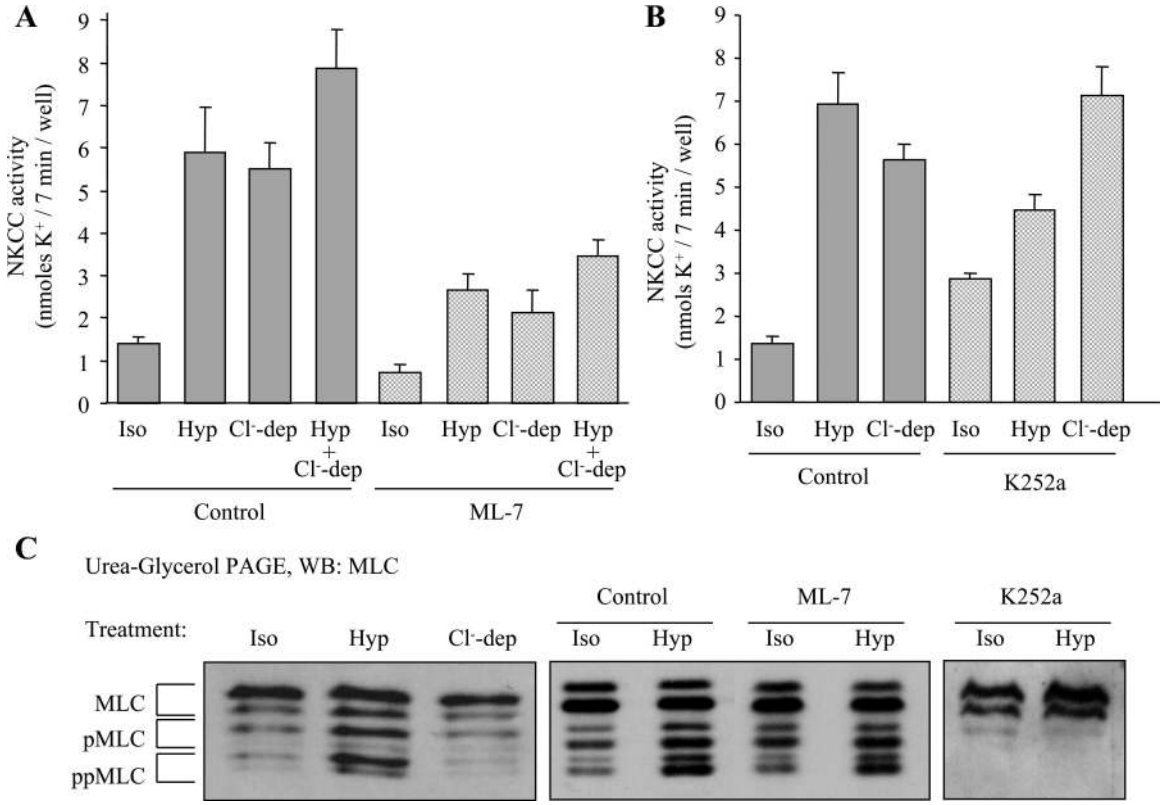

Fig. 2. Differential effect of ML-7 and K252a on NKCC activation and myosin light-chain (MLC) phosphorylation. *A* and *B*: NKCC activity. LLC-PK1 cells were incubated in Iso NaCl in the presence or absence of 75 μM ML-7 or 5 μM K252a for 10 min and treated with Iso NaCl or Cl^--free isotonic sodium methane sulfonic acid (Iso NaMSA; for Cl^- depletion, Cl^--dep) for an additional 30 min in the presence of the same inhibitor concentrations. The media were then replaced with Cl^--containing Iso NaCl that was either isotonic (for Iso and Cl^--dep) or hypertonic (+100 mM sucrose; for Hyp and Hyp + Cl^--dep) for 7 min in the presence of 1.5 μCi ^{86}Rb ($n = 3$). *C*: MLC phosphorylation. LLC-PK1 cells were incubated in Iso NaCl for 30 min in the absence or presence of ML-7 or K252a. Under the same inhibitor conditions, cells were subsequently treated either hypertonically (300 mM sucrose, 20 min) or Cl^- depleted (Iso NaMSA, 30 min) and then lysed. Differentially phosphorylated forms of MLC were separated by performing urea glycerol PAGE, followed by Western blot analysis (WB) for total MLC. The *top two* bands represent nonphosphorylated MLC, the *middle two* bands represent monophosphorylated MLC (pMLC), and the *bottom two* bands represent diphosphorylated MLC (ppMLC). Blot shown is representative of four similar experiments.

motic stress induced a substantial increase in both mono- and diphosphorylated forms of MLC, in accordance with our previous observations (Fig. 2*C*, *left*). In sharp contrast, Cl^- depletion failed to induce any detectable change in the phosphorylation status of MLC (Fig. 2*C*, *left*). The finding that ML-7 suppressed the Cl^- depletion-facilitated NKCC activity, despite the fact that this stimulus does not elicit MLC phosphorylation, not only confirms that ML-7 is not specific for the hyperosmotic activation of NKCC but also suggests that the NKCC-inhibiting effect of ML-7 likely occurs independently of its MLCK-inhibiting action. Furthermore, ML-7 failed to prevent the hyperosmolarity-induced MLC phosphorylation in LLC-PK1 cells (Fig. 2*C*, *middle*) (9). Thus extreme care should be taken when interpreting results based on the use of ML-7, because this drug (at least in epithelial cells) does not appear to be an appropriate tool with which to study the role of MLCK or MLCK-dependent MLC phosphorylation in the hyperosmolarity-induced activation of NKCC.

Differential effects of K525a on basal activity and hyperosmotic or Cl^- depletion-induced activation of NKCC. The above results by no means exclude the potential involvement of MLCK or MLC phosphorylation in the osmotic regulation of NKCC. To better address this issue, we used K252a, a potent and structurally distinct inhibitor of MLCK that has been shown to bind directly to and interfere with MLCK (42). Surprisingly, K252a (5 μM) increased the basal NKCC activity twofold ($P < 0.05$) (Fig. 2*B*), an effect that is in contrast to the inhibitory action of ML-7. Moreover, K252a significantly ($P < 0.01$) reduced the hyperosmosis-induced NKCC activation by ~36% compared with the level of osmotically stimulated transport observed in the absence of the inhibitor. Because K252a increased the basal activity, its inhibitory action is even more pronounced when expressed as a relative increase over the corresponding isotonic transport; hyperosmotic treatment induced a 5.0-fold increase under control conditions, whereas it caused only 1.6-fold activation when K252a was present. Importantly, K252a did not reduce the Cl^- depletion-induced uptake of ^{86}Rb through NKCC, again in contrast to the action of ML-7. Having seen this differential effect, we tested the impact of K252a on basal and hypertonicity-provoked MLC phosphorylation. The drug abolished the basal mono- and diphosphorylation of MLC in resting cells and prevented the increase in phosphorylation upon hypertonic stimulation (Fig. 2*C*, *right*). Taken together, K252a inhibited neither the basal NKCC activity nor the Cl^- depletion-induced activation of the cotransporter, yet it completely suppressed MLC phosphorylation. However, K252a specifically interfered with the hyperosmotic activation of NKCC, suggesting that MLCK (or MLC

Downloaded from journals.physiology.org/journal/ajpcell (106.051.226.007) on August 4, 2022.

phosphorylation) may play a partial role in the hyperosmotic stimulation of the cotransporter.

Novel tools to study the role of MLC phosphorylation in osmotic NKCC activation. MLCK has been shown to alter ion transport through both MLC phosphorylation-dependent and -independent mechanisms (50). Furthermore, whether MLC phosphorylation or merely myosin activity is involved in transporter regulation remains questionable, because the latter can be regulated in a phosphorylation-independent manner as well (14, 54). To approach these issues, we targeted MLC phosphorylation per se rather than MLCK activity. To this end, we applied MLC mutants that mimic the nonphosphorylated or the diphosphorylated MLC. In the nonphosphorylatable mutant (AA-MLC), the target serine and threonine residues were replaced with alanine, whereas in the diphosphorylation-like mutant (DD-MLC), they were exchanged for aspartate (24).

Initially, we tested whether these constructs indeed behave like inactive (and dominant negative) and constitutively active forms of MLC. LLC-PK1 cells were transiently transfected with plasmids encoding Myc-tagged WT-MLC, AA-MLC, or DD-MLC and then immunostained 48 h later using an anti-Myc antibody. As shown in Fig. 3*A* (*left*), WT-MLC showed a fairly even cytosolic distribution, with a few fine fibers and faint peripheral enrichment. Conversely, AA-MLC was mostly cytosolic (Fig. 3*A*, *middle*); however, in nonconfluent monolayers, AA-MLC occasionally localized to fibrous structures at free edges of the cell (data not shown). In contrast, DD-MLC assembled into numerous thick stress fibers and showed some peripheral enrichment (Fig. 3*A*, *right*), similarly to observations in HeLa cells (24). The observation that DD-MLC more readily assembles into fibers suggests that it may be part of functional actomyosin structures and thus behaves like phosphorylated MLC.

Next, we assessed whether AA-MLC could inhibit the phosphorylation of endogenous MLC, thereby acting as a dominant negative. Initially, we wanted to test this possibility independently of any osmotically induced changes; therefore, we took advantage of our previous findings that TGF-β_1 (39) or plasma membrane depolarization by high K^+ (our unpublished results) induce robust MLC phosphorylation in LLC-PK1 cells. To determine whether AA-MLC could inhibit the phosphorylation of endogenous MLC by these stimuli, LLC-PK1 cells were transiently transfected with AA-MLC and subsequently either treated with 4 ng/ml TGF-β_1 for 3 days or acutely exposed to a K^+-based, Ca^{2+}-free solution. Ca^{2+} removal was shown to further potentiate the depolarization-induced MLC phosphorylation (our unpublished results and Ref. 12). Cells were then fixed and immunostained for ppMLC with a ppMLC-specific antibody and for Myc to identify the successfully transfected cells. Under control conditions, total ppMLC staining was weak, with negligible cytosolic labeling and some accumulation in the nucleus (Fig. 3*B*, *top left*) as reported previously (39). Transfection of AA-MLC had no effect on the basal staining, indicating that the ppMLC antibody does not cross react with AA-MLC (Fig. 3*B*, *left*; outlined transfected cells). As expected, TGF-β_1 treatment caused an increase in MLC phosphorylation, which was predominantly visible in central fibrous structures (Fig. 3*B*, *top middle*). Importantly, in cells transfected with AA-MLC (Fig. 3*B*, asterisk), TGF-β_1-induced MLC phosphorylation was entirely prevented (Fig. 3*B*, *middle*). Similarly, the depolarization-induced MLC phosphorylation, which occurred both centrally and at the cell cortex, was dramatically reduced in AA-MLC-transfected cells, albeit the peripheral MLC appeared to be slightly less sensitive to inhibition by AA-MLC (Fig. 3*B*, *right*; outlined transfected cells). Taken together, these results indicate that AA-MLC can be used to interfere with endogenous MLC phosphorylation.

We next assessed the ability of DD-MLC to act as a constitutively active mutant. To this end, we made use of C3 transferase (C3), an enzyme that inactivates Rho by ADP ribosylation, leading to reduced MLC phosphorylation and consequent stress fiber disassembly (6, 28). To determine whether DD-MLC could restore stress fibers in cells in which Rho was inactivated, LLC-PK1 cells were transfected with plasmids encoding C3 and GFP (to identify successfully transfected cells) with or without cotransfection with DD-MLC. Forty-eight hours later, cells were fixed and stained for F-actin using rhodamine-labeled phalloidin. In accordance with our previous results (39), cotransfection with C3 and GFP (asterisk) resulted in the complete loss of stress fibers in 86% (n = 100 cells) of LLC-PK1 cells; that is, only 14% of the cells displayed some stress fibers (Fig. 3*C*, *left*, and graph). However, when cells were triple transfected with DD-MLC, C3, and GFP, stress fiber assembly was rescued, because 74% of the transfected cells (asterisks) contained numerous stress fibers (Fig. 3*C*, *right*, and graph). Collectively, these results indicate that AA-MLC and DD-MLC can behave as dominant negative and constitutively active mutants, respectively, and thus are appropriate tools with which to examine the role of MLC phosphorylation in NKCC activation.

Effect of MLC mutants on osmotic stress-induced MLC phosphorylation and NKCC activation. To assess and quantify the effect of WT-, AA-, and DD-MLC on the hyperosmolarity-induced phosphorylation of endogenous MLC and on NKCC activation, we subcloned these Myc-tagged constructs into a retroviral vector. This approach was necessary because both urea glycerol PAGE and ^{86}Rb uptake are cell population-based assays, which require that a large percentage of the cells express the tested constructs. The efficiency of viral transduction was assessed by immunostaining with an anti-Myc antibody. As shown in (Fig. 4*A*, *top*), confluent monolayers of LLC-PK1 cells were readily infected with each of the three mutants (WT-, AA-, and DD-MLC), consistently resulting in at least 70–80% efficiency. The intracellular distribution of the virally introduced MLC mutants was similar to that of the plasmid-based transfection (Fig. 4*A*, *bottom*).

We then evaluated the ability of AA-MLC to interfere with the hypertonicity-induced MLC phosphorylation. LLC-PK1 cells were either transduced with virus encoding WT-MLC or AA-MLC or left untransduced (Control). Three days later they were treated iso- or hypertonically (+300 mM sucrose), and MLC isoforms were separated using urea glycerol PAGE. To verify expression and assess the behavior of the transfected constructs, the blots were first probed with an anti-Myc antibody. As expected, nontransduced cells did not have any Myc-reactive bands (Fig. 4*B*, *lanes 1* and *2*), whereas LLC-PK1 cells transduced with WT-MLC showed three Myc-reactive bands, indicating that this mutant was effectively mono- and diphosphorylated (Fig. 4*B*, *lanes 3* and *4*). Moreover, hypertonicity induced phosphorylation of WT-MLC, which manifested as a decreased proportion of the nonphosphorylated form and a concomitantly increased proportion of the mono-

Downloaded from journals.physiology.org/journal/ajpcell (106.051.226.007) on August 4, 2022.

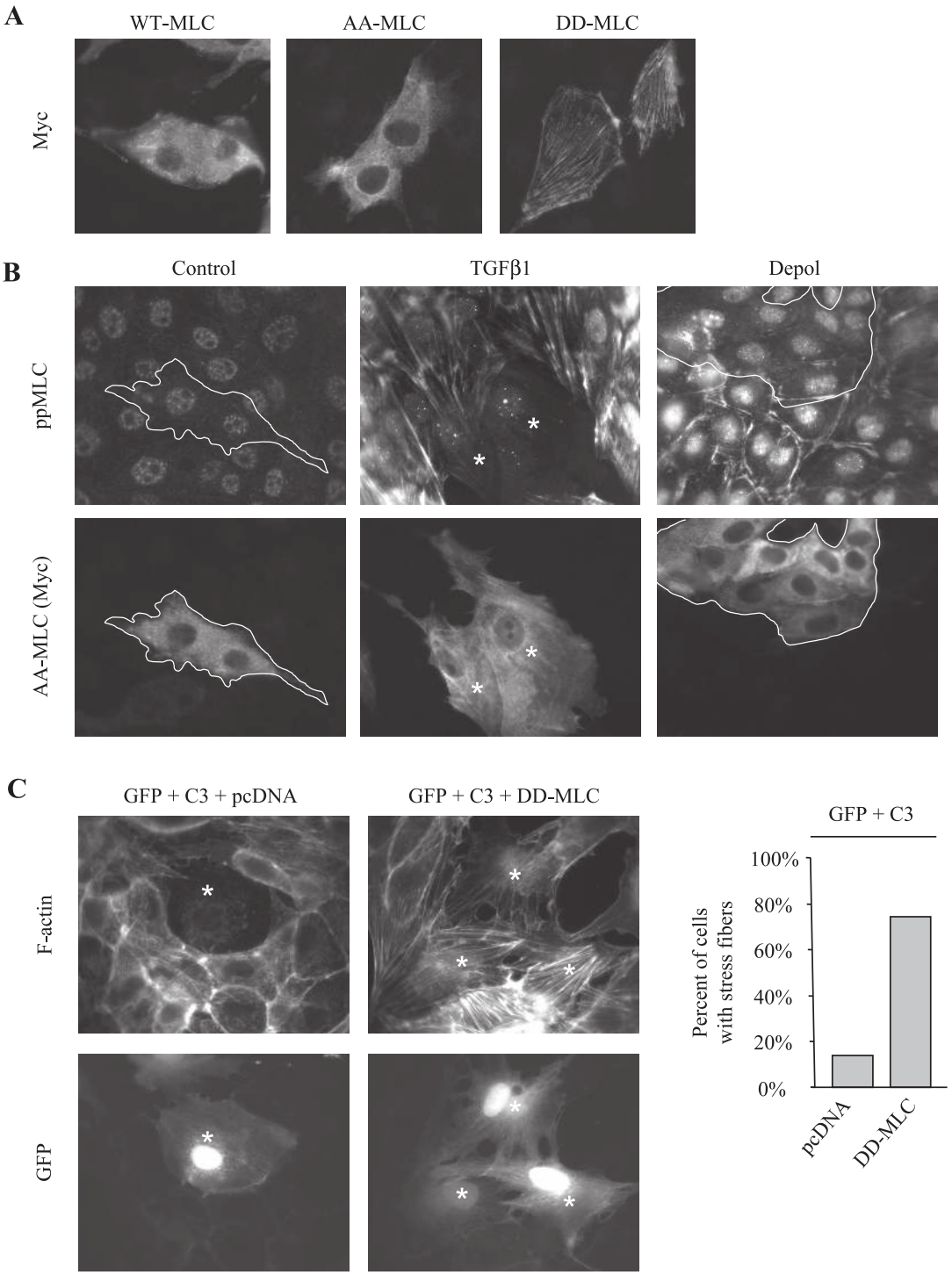

Fig. 3. Characterization of MLC mutants. *A*: subcellular distribution. LLC-PK1 cells were transiently transfected with 1 μg of Myc-tagged wild-type myosin regulatory light chain MRLC2 (WT-MLC) or mutant MRLC2 in which Thr18 and Ser19 were replaced with alanines (AA-MLC) or with aspartic acid (DD-MLC), and 48 h later they were fixed and stained for Myc. *B*: dominant negative effect of AA-MLC on TGF-β_1-induced and membrane depolarization (Depol)-induced MLC phosphorylation. AA-MLC (1 μg) was transiently transfected into LLC-PK1 cells. Six hours after transfection, cells were treated with vehicle (Control and Depol) or with 4 ng/ml TGF-β_1. After an additional 3 days, cells were treated with either Iso NaCl (Control and TGF-β_1) or Iso KCl to induce membrane depolarization (Depol) for 15 min, and subsequently immunostained for ppMLC (*top*) and Myc to identify successfully transfected cells (*bottom*; outline or asterisks indicate the AA-transfected cells). *C*: DD-MLC rescues stress fibers in C3-transferase-transfected cells. LLC-PK1 cells were transfected with plasmids encoding green fluorescent protein (GFP; 0.3 μg) and C3-transferase (1 μg) alone (*right*) or with DD-MLC (1 μg) (*left*). After 48 h, cells were fixed and stained for F-actin using rhodamine-phalloidin (*top*), and successful transfection was indicated by the presence of GFP (*bottom*; asterisks indicate successfully tranfected cells). The percentage of cells with stress fibers was then determined for C3 and C3 + DD-MLC-expressing cells (n = 100 cells for each condition).

Downloaded from journals.physiology.org/journal/ajpcell (106.051.226.007) on August 4, 2022.

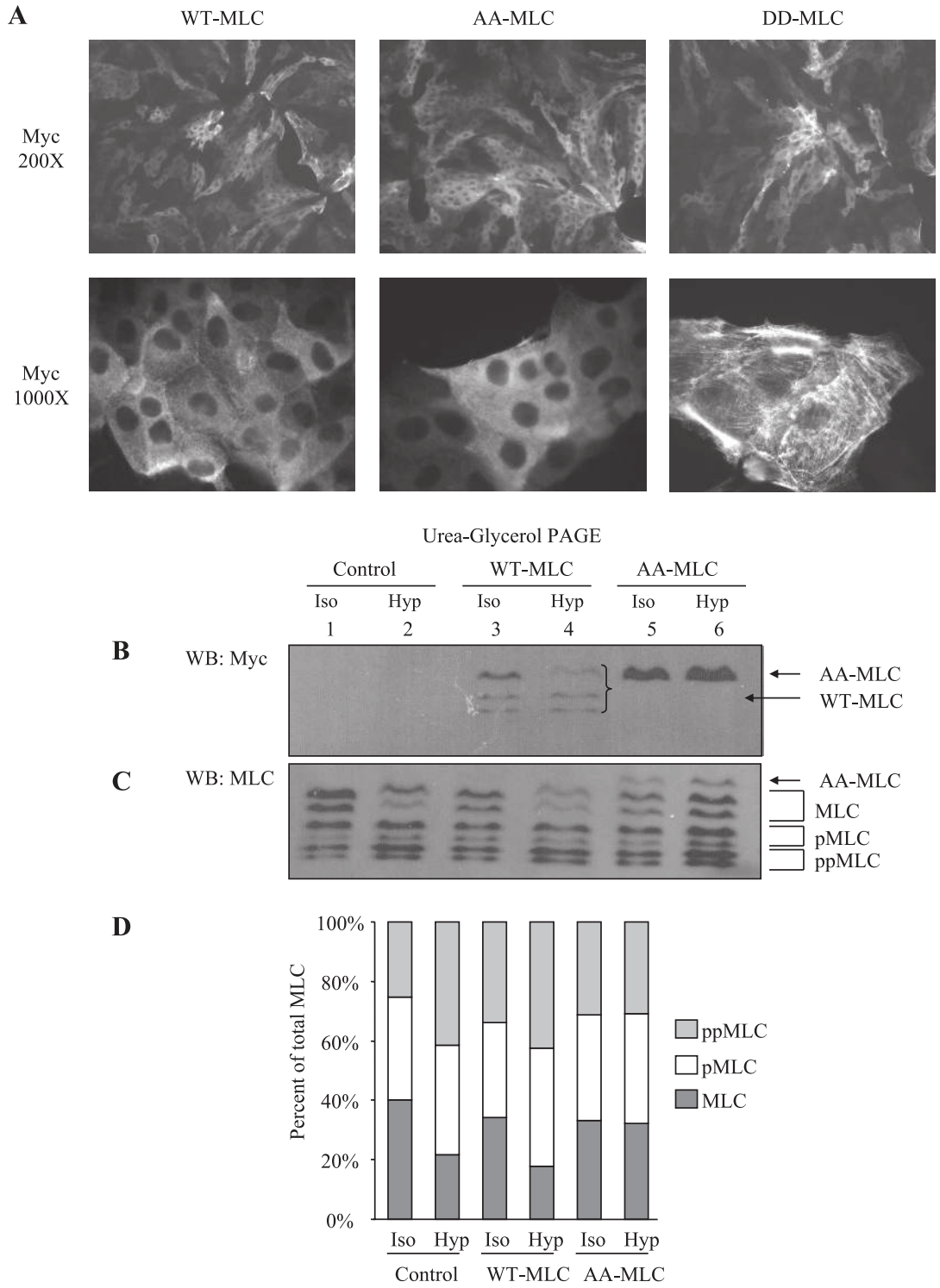

Fig. 4. Viral transduction of LLC-PK1 cells with various MLC mutants. *A*: transduction efficiency of MLC-encoding viruses in LLC-PK1 cells. LLC-PK1 cells were transduced with viral particles encoding WT-, AA-, or DD-MLC, and 48 h later they were immunostained for Myc to identify successfully transduced cells. To assess infection efficiency, Myc staining of confluent monolayers of LLC-PK1 cells is shown at ×200 magnification (*top*). To verify the spatial distribution of virally transduced MLC mutants, islands of LLC-PK1 cells are shown (×1,000 magnification; *bottom*). *B* and *C*: effect of WT-MLC and AA-MLC on the osmotic phosphorylation of endogenous MLC. LLC-PK1 cells were either left untreated or transduced with WT-MLC or AA-MLC. After 48 h, cells were serum starved and treated either isotonically or hypertonically (300 mM sucrose, 20 min). Cells were then lysed, and differentially phosphorylated forms of MLC were separated by performing urea glycerol PAGE. The expression and phosphorylation status of exogenously expressed MLC (i.e., Myc-tagged WT-MLC and AA-MLC) was determined using Western blot analysis with an anti-Myc antibody (*B*). The blot was then reprobed with an MLC antibody that recognizes both Myc-tagged and endogenous MLC (*C*). *D*: percentage of non-, mono-, and diphosphorylated MLC for each condition was determined using densitometric analysis of a representative blot ($n = 3$ experiments) and plotted.

Downloaded from journals.physiology.org/journal/ajpcell (106.051.226.007) on August 4, 2022.

and diphosphorylated forms (Fig. 4*B*, *lanes 3* and *4*). In contrast, LLC-PK1 cells transduced with AA-MLC showed only one Myc-reactive band, which migrated close to the nonphosphorylated WT-MLC and showed no change after hypertonic exposure. (Fig. 4*B*, *lanes 5* and *6*). The blots were then reprobed with anti-MLC antibody, which detects both endogenous and Myc-tagged MLC (Fig. 4*C*), and the amount of non-, mono-, and diphosphorylated forms in each lane was determined and plotted as a percentage of the total MLC (Fig. 4*D*). It is noteworthy that the Myc-tagged WT-MLC comigrated with endogenous MLC, thus this determination reflects the changes in total MLC phosphorylation. In contrast, AA-MLC clearly migrated above the six endogenous bands normally present, thereby allowing us to determine its effect on endogenous MLC. As expected, in untransduced cells, endogenous MLC was both mono- and diphosphorylated by hypertonicity (Fig. 4, *C* and *D*, *lanes 1* and *2*). Interestingly, under isotonic conditions, cells transduced with either WT-MLC or AA-MLC exhibited a slight increase in diphosphorylated MLC compared with untransduced controls (Fig. 4, *C* and *D*, *lanes 3* and *5*). Nonetheless, in cells expressing WT-MLC, osmotic stress was still able to cause a decrease in nonphosphorylated MLC and an increase in diphosphorylated MLC, indicating that WT-MLC did not interfere with the hypertonic effect (Fig. 4, *C* and *D*, *lanes 3* and *4*). In contrast, in cells transduced with AA-MLC, hypertonicity failed to induce a change in the relative amounts of non-, mono-, and diphosphorylated MLC, suggesting that AA-MLC effectively inhibited the hypertonic MLC response (Fig. 4, *C* and *D*, *lanes 5* and *6*).

Next, we tested the effects of the MLC mutants on basal and stimulated NKCC activity. LLC-PK1 cells were either untreated (Control) or infected with WT-, AA-, or DD-MLC, and 3 days later NKCC activity was determined under isotonic and hypertonic conditions. As shown in Fig. 5, hypertonicity increased the rate of NKCC activity 5.1-fold in untransduced control cells (Control). A similar effect was observed in WT-MLC infected cells, indicating that the presence of exogenously supplied MLC does not interfere with the basal NKCC activity or its hypertonic stimulation (WT-MLC, Fig. 5). In AA-MLC-expressing cells, the basal (isotonic) NKCC activity was slightly elevated, although this was not significantly different from control or WT-MLC-expressing cells (Fig. 5). Importantly, in AA-MLC-expressing cells, hyperosmolarity remained able to stimulate NKCC to the same level observed in nontransduced or WT-MLC-expressing cells (AA-MLC, Fig. 5). Finally, transduction with DD-MLC failed to significantly increase NKCC activity, suggesting that DD-MLC is insufficient to activate NKCC (DD-MLC, Fig. 5). Furthermore, in the presence of DD-MLC, the hyperosmotic NKCC activity reached the same level as that of control cells (DD-MLC, Fig. 5). Taken together, these results show that while AA-MLC can suppress hyperosmotically induced MLC phosphorylation, it has no significant effect on hyperosmotic NKCC activation. Furthermore, expression of DD-MLC, which mimics phosphorylated MLC, does not in itself activate NKCC and cannot potentiate hyperosmolarity-induced activation of NKCC. These results suggest that MLC phosphorylation per se is neither required nor sufficient for hyperosmotic NKCC activation.

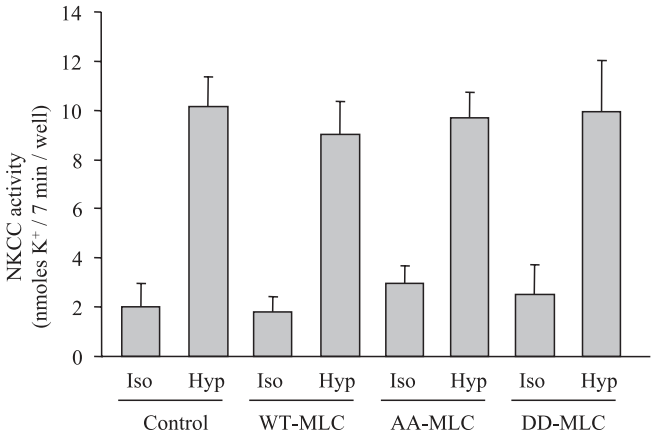

Fig. 5. The effect of MLC mutants on basal and hyperosmotically stimulated NKCC activity. LLC-PK1 cells were either left untreated (Control) or transduced with viral particles encoding WT-, AA-, or DD-MLC, and 72 h later, the bumetanide-sensitive ^{86}Rb uptake was determined under isotonic and hypertonic conditions ($n = 3$). One-way ANOVA showed that none of the isotonic values were significantly different from each other and that none of the hypertonic values were significantly different from each other. $P > 0.05$.

Induction of cortical MLC phosphorylation is not sufficient for NKCC activation. Next, we asked whether an increase in endogenous myosin phosphorylation could affect NKCC. We also considered that the MLC mutants might not efficiently distribute in all MLC pools. Because NKCC is likely to be affected by near-membrane (i.e., peripheral) MLC pools, we wished to test the effect of elevated peripheral MLC phosphorylation on NKCC. Uncoupling of cell-cell contacts by removal of extracellular Ca^{2+} has been shown to induce peripheral MLC accumulation and phosphorylation in epithelial cells (12, 23), and our data show that this phenomenon is present in LLC-PK1 cells as well. Indeed, there was very little ppMLC in the cytosol or at the periphery in control cells, while Ca^{2+} removal resulted in a robust accumulation of ppMLC at the cell periphery (Fig. 6, *A* and *B*). In parallel experiments, we determined NKCC activity under the same conditions. As shown in Fig. 6*C*, Ca^{2+} removal had no significant effect on NKCC activity, strongly suggesting that peripheral MLC phosphorylation in itself is insufficient to activate the cotransporter. The lack of activation was not due to a Ca^{2+} removal-induced suppression of transporter activity, because NKCC remained responsive to, and was markedly activated by, hypertonic stress after Ca^{2+} removal (Fig. 6*C*).

To assess the mechanism underlying peripheral MLC phosphorylation upon Ca^{2+} removal, we tested the effect of various inhibitors on this process. ML-7 did not prevent the rise in MLC phosphorylation (Fig. 6*D*), while both the ROK inhibitor Y-27632 and the Rho family inhibitor *Clostridium* toxin B abolished this response (Fig. 6, *E* and *F*). This suggests that the ensuing peripheral MLC phosphorylation was mediated by the ROK pathway. These data further substantiate the dissociation between peripheral MLC phosphorylation and NKCC regulation. Specifically, ML-7 inhibited NKCC but did not reduce peripheral MLC phosphorylation, whereas Y-27632 and *Clostridium* toxin B, which were able to prevent peripheral MLC phosphorylation, had no effect on basal or hyperosmotically induced NKCC activity (9) (not shown for *Clostridium* toxin B).

Myosin ATPase activity contributes to hyperosmotic regulation of NKCC. MLCK has been shown to influence myosin ATPase activity in a MLC phosphorylation-independent fash-

Downloaded from journals.physiology.org/journal/ajpcell (106.051.226.007) on August 4, 2022.

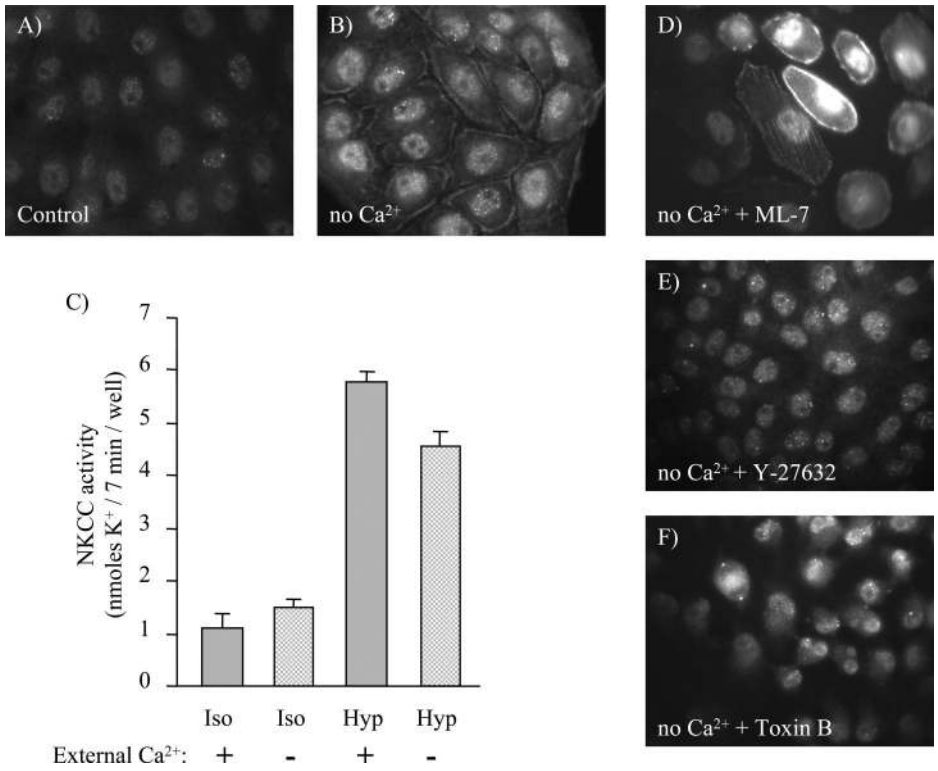

Fig. 6. Induction of peripheral MLC phosphorylation fails to induce NKCC activation. Ca^{2+} removal-induced peripheral MLC phosphorylation, and the effect of various inhibitors on the process is shown. LLC-PK1 cells were preincubated in Iso NaCl containing vehicle (*A* and *B*), 75 μM ML-7 (*D*), 20 μM Y-27632 (*E*), or 0.8 μg/ml *Clostridium* toxin B (*F*) for 30 min. *F*: 0.8 μg/ml *Clostridium* toxin B was already present during serum deprivation until cell rounding was achieved (~2–3 h). Subsequently, cells were either left untreated (*A*) or exposed to Ca^{2+}-free Iso NaCl for 15 min (*B* and *D–F*) in the presence of vehicle or under the same inhibitor conditions. Cells were then fixed and immunostained using a ppMLC-specific antibody. *C*: effect of external Ca^{2+} removal on basal and osmotically stimulated NKCC activity. LLC-PK1 cells were incubated in Ca^{2+}-containing (+) or Ca^{2+}-free (−) medium for 5 min. Subsequently, NKCC activity was determined as the bumetanide-sensitive cellular uptake of ^{86}Rb under isotonic or hypertonic conditions in the presence (+) or absence (−) of external Ca^{2+}. A representative sample of two separate experiments performed in triplicate is shown.

ion (14, 54) by directly binding to the myosin heavy chain and stimulating myosin ATPase activity. Furthermore, while an increase in myosin phosphorylation is not the signal for enhanced NKCC activity, a basal level of myosin activity may be a necessary permissive factor for the hypertonic response. To examine this possibility, we used blebbistatin, a novel and highly specific inhibitor of myosin II ATPase activity (33, 52). To determine whether blebbistatin effectively penetrated the cells, we initially performed F-actin staining. Blebbistatin caused a dramatic reduction in the number of stress fibers and induced a relaxed cell morphology, which manifested as a longer and convoluted actin rim at the cell perimeter (Fig. 7*A*). Next, we tested the effect of the drug on the osmotic and Cl^- depletion-induced NKCC activation. As shown in Fig. 7*B*, blebbistatin did not significantly alter the basal activity of NKCC. Importantly, it reduced hypertonicity-induced NKCC activation by 38% ($P < 0.001$), while it had no effect on Cl^- depletion-induced activation (Fig. 7*B*). Interestingly, MLCK inhibition using K252a, which abolished basal MLC phosphorylation, showed the same effect as blebbistatin in that both compounds specifically, and to a similar extent, inhibited the hyperosmolarity-induced NKCC activity. These findings suggest that myosin ATPase activity is a significant factor in the osmotic regulation of NKCC, and they are consistent with the possibility that MLCK may regulate NKCC activity by directly regulating myosin ATPase activity.

Previous studies have shown that, in certain cell types, the F-actin skeleton plays an important role in the regulation of NKCC upon osmotic (20, 41) or hormonal stimulation (32, 34, 40). Because blebbistatin induced stress fiber disassembly and therefore a major change in the actin skeleton, it was conceivable that its effect on the transport was not directly due to the inhibition of the myosin ATPase, but rather to the consequent disruption of the actin skeleton. To address this possibility, we treated the cells with latrunculin B (LatB), a potent actin monomer-sequestering agent that was shown to inhibit NKCC activation in lung epithelial cells (32). LatB caused gross F-actin depolymerization that manifested in the elimination of stress fibers and a drastic decrease in the intensity of the peripheral F-actin ring (Fig. 7*A*). Despite these robust cytoskeletal changes, LatB affected neither the basal activity of NKCC nor its hyperosmotic stimulation (Fig. 7*C*). Similar results were obtained when the cytoskeleton was disrupted with *Clostridium* toxin B, a potent inhibitor of Rho, Rac, and Cdc42 (not shown). Thus, although these Rho family GTPases are stimulated by hyperosmolarity (8, 9, 30), our results indicate that neither their activity nor overall cytoskeletal integrity is required for the osmotic stimulation of NKCC in LLC-PK1 cells. These observations also imply that the inhibitory action of blebbistatin was not due to alterations in F-actin. On the other hand, our findings do not exclude the possibility that remaining peripheral F-actin structures, which may be less affected by the applied pharmacological agents, participate in the maintenance of localized, actomyosin-based contractility.

LLC-PK1 cells express mRNA for both NKCC1 and NKCC2. Because LLC-PK1 cells are derived from the kidney and have been reported to contain NKCC activity in their apical (brush border) membrane (5), we wondered which cotransporter isoforms they might express. Because the commercially available antibodies produced poor labeling in LLC-PK1 cells, we sought to gain some insight into this question by performing RT-PCR (Fig. 8). We designed isoform-specific primers on the basis of the alignment of human, rat, and mouse sequences for NKCC1 and NKCC2. With the use of these probes, the message for both NKCC1 and NKCC2 was clearly detected in murine kidney, a tissue that served as a positive control.

Downloaded from journals.physiology.org/journal/ajpcell (106.051.226.007) on August 4, 2022.

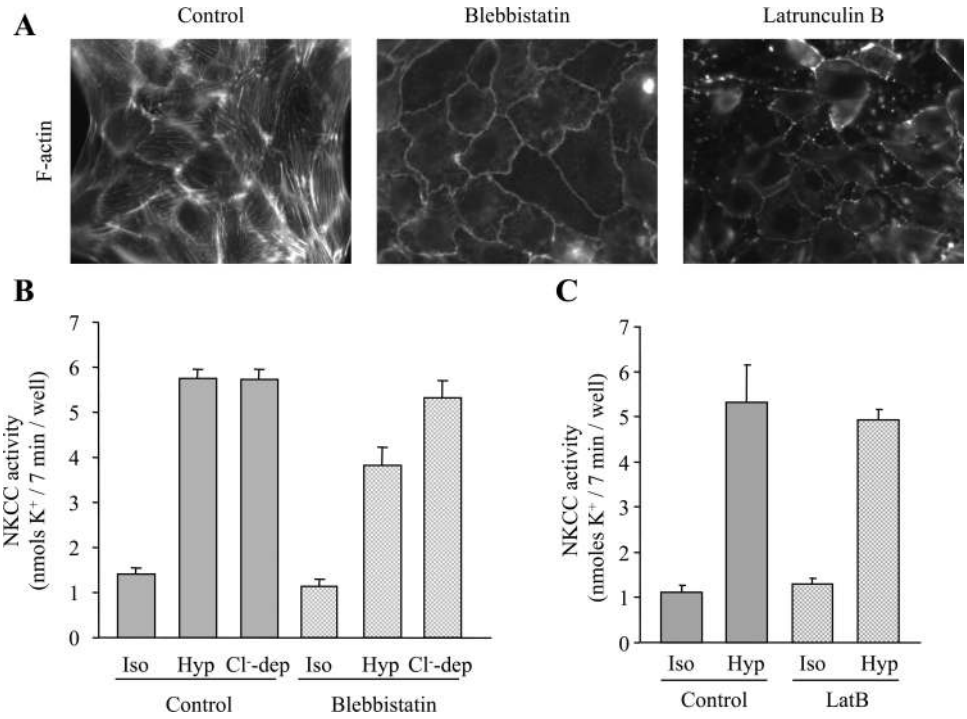

Fig. 7. Inhibition of myosin II ATPase using blebbistatin reduces osmotic activation of NKCC, independent of stress fiber disassembly. Serum-deprived LLC-PK1 cells were preincubated in Iso NaCl in either the absence (Control) or the presence of blebbistatin (100 μM) or latrunculin B (LatB; 5 μM) for 30 min. In *A* and *B*, blebbistatin was already present during serum deprivation. *A*: cells were stained for F-actin using rhodamine-phalloidin. *B* and *C*: cells were incubated in Iso NaCl or Iso NaMSA for 30 min under the same inhibitor conditions. Subsequently, cells were incubated in Cl^--containing medium that was either isotonic (Iso and Cl^--dep) or hypertonic (Hyp) while maintaining the same inhibitor concentrations, and bumetanide-sensitive ^{86}Rb uptake was determined (*B* and *C*; $n = 3$).

Importantly, LLC-PK1 cells also contained mRNA for both NKCC1 and NKCC2. In contrast, only NKCC1 mRNA was present in PAECs as well as in MEFs. As a loading control, β-actin RT-PCR was performed, which showed comparable message levels in each sample (Fig. 8). Collectively, these data show that our probes were able to specifically amplify NKCC1 and NKCC2 from both murine and porcine tissues and that LLC-PK1 cells express both isoforms at the mRNA level. Clearly, future studies are warranted to establish whether (and if so, to what extent) NKCC2 might contribute to the apical NKCC activity in LLC-PK1 cells (see DISCUSSION).

DISCUSSION

The central aim of the present study was to examine the role of MLC phosphorylation in the osmotic regulation of NKCC. On the basis of pharmacological and genetic approaches, which either induce or mimic MLC phosphorylation, our results clearly indicate that an increase in MLC phosphorylation itself is not a sufficient trigger to activate NKCC in kidney tubular cells. Moreover, prevention of the hypertonicity-induced increase in endogenous MLC phosphorylation by a dominant negative form of MLC did not reduce the osmotic stimulation of NKCC, providing further evidence that a net rise in MLC phosphorylation is not necessary for the effect. On the other hand, basal myosin ATPase activity proved to be a requirement for the maximal stimulation of NKCC by hyperosmotic stress, indicating a permissive role for the contractile apparatus in the regulation of the cotransporter.

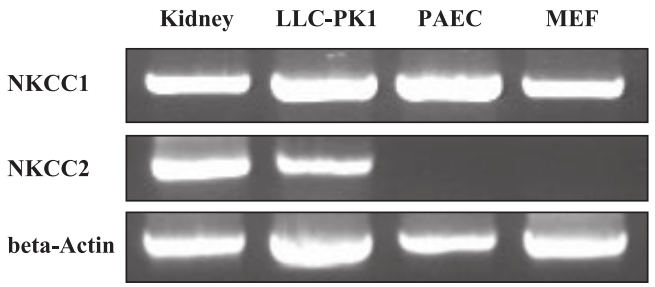

Fig. 8. LLC-PK1 cells contain mRNA for both NKCC1 and NKCC2. Total mRNA was isolated from mouse kidney, LLC-PK1 cells, porcine aortic endothelial cells (PAEC), and mouse embryonic fibroblasts (MEF). RT-PCR was then performed using primers specific for NKCC1, NKCC2, and β-actin.

These conclusions may appear somewhat surprising because previous reports from several laboratories, including our own, have shown that the MLCK inhibitor ML-7 or ML-9 reduced the osmotic (9, 26, 27) or agonist-induced (1, 20) activation of NKCC. Indeed, the notion of the contractile regulation of NKCC stemmed from such pharmacological studies. However, several observations support the concept that the ML-7-induced inhibition of NKCC is not (or is not exclusively) due to the inhibition of MLCK-mediated MLC phosphorylation. The dose of ML-7 required to achieve maximal inhibition ranged from <1 μM to >100 μM, depending on the cell type tested. Because the K_i of ML-7 for MLCK is 0.3 μM, results obtained at near-micromolar doses (e.g., in Ehrlich ascites cells; Ref. 27) likely reflect an MLCK-dependent effect. However, this result is doubtful at higher concentrations, at which the drug is known to affect a variety of other kinases, including PKA ($IC_{50} = 21$ μM) and PKC ($IC_{50} = 42$ μM) (as listed in the Biomol catalog; see also Refs. 25, 49). Importantly, our data provide direct evidence that in LLC-PK1 cells, ML-7 exerts its effect independently of MLC phosphorylation. First, ML-7 inhibited the hypertonicity-induced and Cl^- depletion-triggered NKCC activation equally, despite the fact that Cl^- depletion (as opposed to hypertonicity) did not provoke any MLC phosphorylation. Second, ML-7 reduced the basal NKCC activity as well, without inducing a decrease in basal MLC phosphorylation. This effect is in contrast to that of K252a, which abolished basal MLC phosphorylation without reducing

Downloaded from journals.physiology.org/journal/ajpcell (106.051.226.007) on August 4, 2022.

either the basal or the Cl^- depletion-enhanced activity of the cotransporter; however, it specifically inhibited the hypertonic stimulation of NKCC. In addition, blebbistatin, a direct and specific inhibitor of myosin ATPase (33, 52), also failed to affect basal or Cl^- depletion-induced transport, while it partially inhibited the hypertonic effect. Finally, it is noteworthy that the maximal (~60%) inhibition exerted by ML-7 was significantly higher than the reduction (~35%) obtained after total inhibition of basal MLC phosphorylation or the myosin ATPase. The latter observation also implies that a substantial portion of the osmotic NKCC activation is entirely independent of myosin.

Clearly, in our cellular setting, ML-7 affects NKCC regulation through factors other than MLC phosphorylation. Consistent with this idea is the hypothesis that ML-7 might influence putative volume sensitive kinases because it activated the K^+-Cl^- cotransporter (KCC), a swelling-stimulated ion translocator, apparently in an MLCK-independent fashion (25). Because KCC is regulated by a swelling-inactivated kinase and can also bind to PASK (46), it is conceivable that PASK or similar kinases might be sensitive to ML-7. An argument against this possibility is that ML-7 was reported not to inhibit the total level of NKCC phosphorylation (26). However, an important complicating factor in the interpretation of these data is that ML-7 in itself strongly increased NKCC phosphorylation under isotonic conditions (26). This finding implies that ML-7 may indeed modify NKCC phosphorylation. Because the individual target threonine and serine residues, some of which may be stimulatory or inhibitory (11, 35), have not been identified, future studies are required to clarify the functional significance of this phenomenon. Regrettably, we were unable to precipitate NKCC from LLC-PK1 cells efficiently with the available antibodies. Nonetheless, regardless of the underlying mechanism, these observations verify that NKCC inhibition obtained by high ML-7 concentrations cannot be accounted for by an inhibitory action on MLC phosphorylation.

In principle, two major factors may be responsible for the differential inhibitor sensitivity of the hyperosmotic stimulation of NKCC in various cells: differences in the signaling pathways relaying osmostress to the cotransporter and/or differences in the cotransporter isoform being affected by these pathways. Regarding the first possibility, it is very likely that the relative contribution of MLCK to MLC phosphorylation varies greatly in different tissues. For example, in LLC-PK1 cells, the ROK pathway appears to be the primary, although not the exclusive, determinant of overall MLC phosphorylation (9, 39). It is conceivable, however, that in Ehrlich ascites cells, MLCK has a predominant role, and therefore its inhibition could reduce basal MLC phosphorylation and thus myosin ATPase activity to a subthreshold level that is insufficient to maintain a permissive effect for osmotic activation.

Previously, the contractile regulation of NKCC was studied in cells that express NKCC1 exclusively. Our data show that, at least at the mRNA level, LLC-PK1 cells express NKCC2 as well. Interestingly, LLC-PK1 cells have been shown to contain apically localized (brush border) NKCC activity (5). Because our transport measurements were conducted on confluent monolayers with ^{86}Rb added from the apical side, it seems probable that apical cotransporters significantly contributed to the measured unidirectional ion flux. While these findings are consistent with the possibility that NKCC2 might participate in the measured cotransporter activity, it remains to be established whether the apical cotransporter of LLC-PK1 cells is indeed NKCC2. Similarly, future studies are warranted to address whether the permissive (as opposed to signaling) role of myosin described herein is a property of both isoforms or is a characteristic of NKCC2.

The limitations of the pharmacological approaches prompted us to investigate the role of myosin phosphorylation by cell biological means as well. This was achieved with the use of myosin mutants that are either nonphosphorylatable (AA-MLC) or mimic the diphosphorylated form (DD-MLC). AA-MLC has been shown to inhibit cell migration in HeLa cells and was proposed to act both by replacing the normal MLC in myosin and by inhibiting MLCK (13). We verified that AA-MLC acts as a potent dominant negative construct in LLC-PK1 cells, because it abrogated MLC phosphorylation induced by TGF-β_1, depolarization, or hyperosmolarity. However, AA-MLC (similar to WT-MLC) did not suppress, and in fact slightly elevated, basal MLC phosphorylation, an effect that might be due to its interference with myosin phosphatase. We also showed that DD-MLC functions as a constitutively active construct, because it was able to prevent the cytoskeleton-disrupting effects of Rho inactivation. Nonetheless, AA- or DD-MLC did not interfere with the basal or osmotic activity of NKCC. These findings, together with our previous observation that ROK inhibition drastically reduces MLC phosphorylation yet has no effect on NKCC activation (9), provide strong support for the concept that an increase in MLC phosphorylation is not a trigger for osmotic cotransporter activation.

Nonetheless, it remained plausible that a basal level of myosin-dependent contractility could play a permissive role in the shrinkage-induced cotransporter activation. Indeed, this notion was supported by our findings that the myosin II ATPase inhibitor blebbistatin reduced the osmotic activation of NKCC by 35% and that the total abolition of MLC phosphorylation by K252a was accompanied by a similar reduction in hypertonic transport. Importantly, neither treatment reduced the isotonic NKCC activity. If MLCK activity is a necessary upstream component of this effect, it may contribute to contractility via two mechanisms. First, MLCK may maintain a basal level of phosphorylation of a small pool of MLC near the plasma membrane. However, this MLC pool must be ROK independent and unavailable to inhibition by AA-MLC. This possibility cannot be excluded fully, because AA-MLC, which abolished central MLC phosphorylation by TGF-β_1 treatment, appeared to be slightly less effective at inhibiting peripheral MLC phosphorylation induced by depolarization. Alternatively, MLCK may bypass MLC phosphorylation and act directly on myosin. This possibility is supported by findings that MLCK can bind directly to myosin II and stimulate its ATPase activity (14, 54). Conceivably, MLCK may influence NKCC activity directly as reported for a Ca^{2+} channel (50). However, this mechanism is less likely, because myosin activity proved to be involved in osmotic cotransporter activation.

The mechanism whereby myosin activity contributes to the maintenance of the osmotic sensitivity of NKCC remains to be elucidated. Myosin activity may help to keep NKCC in a responsive conformation or may provide a cytoskeletal structure necessary for the docking of NKCC-regulatory factors.

Finally, because the various pharmacological agents could affect non-MLC-related signaling events as well (e.g., K252a

Downloaded from journals.physiology.org/journal/ajpcell (106.051.226.007) on August 4, 2022.

also inhibits PKC and PKA), we should briefly consider their potential involvement. PKC has been implicated in osmotic NKCC1 stimulation (21, 31), presumably upstream of ERK (31, 55). However, in LLC-PK1 cells, inhibition of ERK activation by PD-98059 had no effect on the osmotic stimulation of NKCC (data not shown). PKA was reported to inhibit NKCC2 (29), which may account for the stimulatory effect of K252a on basal transport, but not for the inhibitory effect on hypertonic stimulation. Importantly, both ML-7 and K252a might influence calmodulin (CaM)-dependent signaling, which also was implicated in NKCC regulation (27). However, hypertonicity does not significantly alter cytosolic Ca^{2+} (43), and chelation of intracellular Ca^{2+} by BAPTA did not alter the hypertonic ^{86}Rb uptake in our cells (data not shown), in agreement with earlier findings in endothelium (43). Nonetheless, Ca^{2+}-independent, tyrosine phosphorylation-mediated activation of CaM and its subsequent binding to the Na^+/H^+ exchanger type 1 (NHE1) has been described as a prime mechanism for the osmotic activation of NHE1. Interestingly, a high concentration of ML-7 blocks the osmotic NHE1 activation as well (51), in a presumably MLCK-independent manner (15). Direct activation of NKCC by CaM should be considered an attractive candidate mechanism because both NKCC1 and NKCC2 have putative CaM-binding sites, and our preliminary data suggest that CaM translocates to the cell periphery upon osmotic shock. Future studies should test the hypothesis that the alternative CaM activation represents an ML-7-sensitive yet MLCK-independent mechanism involved in the osmotic regulation of NKCC isoforms.

ACKNOWLEDGMENTS

We thank Shao-Wei Huang for valuable contributions to the experiments.

GRANTS

This work was supported by grants from the Canadian Institutes of Health Research (CIHR) and from the Natural Sciences and Engineering Research Council of Canada (to A. Kapus). C. Di Ciano-Oliveira is a recipient of a Canada Graduate Scholarship from CIHR. K. Szászi is a CIHR senior research fellow.

REFERENCES

1. **Akar F, Jiang G, Paul RJ, and O'Neill WC.** Contractile regulation of the Na^+-K^+-$2Cl^-$ cotransporter in vascular smooth muscle. *Am J Physiol Cell Physiol* 281: C579–C584, 2001.
2. **Arthur WT and Burridge K.** RhoA inactivation by p190RhoGAP regulates cell spreading and migration by promoting membrane protrusion and polarity. *Mol Biol Cell* 12: 2711–2720, 2001.
3. **Bain J, McLauchlan H, Elliott M, and Cohen P.** The specificities of protein kinase inhibitors: an update. *Biochem J* 371: 199–204, 2003.
4. **Breitwieser GE, Altamirano AA, and Russell JM.** Elevated $[Cl^-]_i$ and $[Na^+]_i$ inhibit Na^+,K^+,Cl^- cotransport by different mechanisms in squid giant axons. *J Gen Physiol* 107: 261–270, 1996.
5. **Brown CD and Murer H.** Characterization of a Na : K : 2Cl cotransport system in the apical membrane of a renal epithelial cell line (LLC-PK1). *J Membr Biol* 87: 131–139, 1985.
6. **Chrzanowska-Wodnicka M and Burridge K.** Rho-stimulated contractility drives the formation of stress fibers and focal adhesions. *J Cell Biol* 133: 1403–1415, 1996.
7. **Darman RB and Forbush B.** A regulatory locus of phosphorylation in the N terminus of the Na-K-Cl cotransporter, NKCC1. *J Biol Chem* 277: 37542–37550, 2002.
8. **Di Ciano C, Nie Z, Szászi K, Lewis A, Uruno T, Zhan X, Rotstein OD, Mak A, and Kapus A.** Osmotic stress-induced remodeling of the cortical cytoskeleton. *Am J Physiol Cell Physiol* 283: C850–C865, 2002.
9. **Di Ciano-Oliveira C, Sirokmány G, Szászi K, Arthur WT, Masszi A, Peterson M, Rotstein OD, and Kapus A.** Hyperosmotic stress activates Rho: differential involvement in Rho kinase-dependent MLC phosphorylation and NKCC activation. *Am J Physiol Cell Physiol* 285: C555–C566, 2003.
10. **Dowd BFX and Forbush B.** PASK (proline-alanine-rich STE20-related kinase), a regulatory kinase of the Na-K-Cl cotransporter (NKCC1). *J Biol Chem* 278: 27347–27353, 2003.
11. **Flatman PW.** Regulation of Na-K-2Cl cotransport by phosphorylation and protein-protein interactions. *Biochim Biophys Acta* 1566: 140–151, 2002.
12. **Frixione E, Lagunes R, Ruiz L, Urbán M, and Porter RM.** Actin cytoskeleton role in the structural response of epithelial (MDCK) cells to low extracellular Ca^{2+}. *J Muscle Res Cell Motil* 22: 229–242, 2001.
13. **Fumoto K, Uchimura T, Iwasaki T, Ueda K, and Hosoya H.** Phosphorylation of myosin II regulatory light chain is necessary for migration of HeLa cells but not for localization of myosin II at the leading edge. *Biochem J* 370: 551–556, 2003.
14. **Gao Y, Kawano K, Yoshiyama S, Kawamichi H, Wang X, Nakamura A, and Kohama K.** Myosin light chain kinase stimulates smooth muscle myosin ATPase activity by binding to the myosin heads without phosphorylating the myosin light chain. *Biochem Biophys Res Commun* 305: 16–21, 2003.
15. **Garnovskaya MN, Mukhin YV, Vlasova TM, and Raymond JR.** Hypertonicity activates Na^+/H^+ exchange through Janus kinase 2 and calmodulin. *J Biol Chem* 278: 16908–16915, 2003.
16. **Haas M and Forbush B III.** The Na-K-Cl cotransporter of secretory epithelia. *Annu Rev Physiol* 62: 515–534, 2000.
17. **Haas M and Forbush B III.** The Na-K-Cl cotransporters. *J Bioenerg Biomembr* 30: 161–172, 1998.
18. **Haas M, McBrayer D, and Lytle C.** $[Cl^-]_i$-dependent phosphorylation of the Na-K-Cl cotransport protein of dog tracheal epithelial cells. *J Biol Chem* 270: 28955–28961, 1995.
19. **Hebert SC, Mount DB, and Gamba G.** Molecular physiology of cation-coupled Cl^- cotransport: the SLC12 family. *Pflügers Arch* 447: 580–593, 2004.
20. **Hecht G and Koutsouris A.** Myosin regulation of NKCC1: effects on cAMP-mediated Cl^- secretion in intestinal epithelia. *Am J Physiol Cell Physiol* 277: C441–C447, 1999.
21. **Heinzinger H, van den Boom F, Tinel H, and Wehner F.** In rat hepatocytes, the hypertonic activation of Na^+ conductance and Na^+-K^+-$2Cl^-$ symport—but not Na^+-H^+ antiport—is mediated by protein kinase C. *J Physiol* 536: 703–715, 2001.
22. **Isenring P, Jacoby SC, Payne JA, and Forbush B III.** Comparison of Na-K-Cl cotransporters: NKCC1, NKCC2, and the HEK cell Na-K-Cl cotransporter. *J Biol Chem* 273: 11295–11301, 1998.
23. **Ivanov AI, McCall IC, Parkos CA, and Nusrat A.** Role for actin filament turnover and a myosin II motor in cytoskeleton-driven disassembly of the epithelial apical junctional complex. *Mol Biol Cell* 15: 2639–2651, 2004.
24. **Iwasaki T, Murata-Hori M, Ishitobi S, and Hosoya H.** Diphosphorylated MRLC is required for organization of stress fibers in interphase cells and the contractile ring in dividing cells. *Cell Struct Funct* 26: 677–683, 2001.
25. **Kelley SJ, Thomas R, and Dunham PB.** Candidate inhibitor of the volume-sensitive kinase regulating K-Cl cotransport: the myosin light chain kinase inhibitor ML-7. *J Membr Biol* 178: 31–41, 2000.
26. **Klein JD and O'Neill WC.** Volume-sensitive myosin phosphorylation in vascular endothelial cells: correlation with Na-K-2Cl cotransport. *Am J Physiol Cell Physiol* 269: C1524–C1531, 1995.
27. **Krarup T, Jakobsen LD, Jensen BS, and Hoffmann EK.** Na^+-K^+-$2Cl^-$ cotransport in Ehrlich cells: regulation by protein phosphatases and kinases. *Am J Physiol Cell Physiol* 275: C239–C250, 1998.
28. **Kreisberg JI, Ghosh-Choudhury N, Radnik RA, and Schwartz MA.** Role of Rho and myosin phosphorylation in actin stress fiber assembly in mesangial cells. *Am J Physiol Renal Physiol* 273: F283–F288, 1997.
29. **Laamarti MA, Bell PD, and Lapointe JY.** Transport and regulatory properties of the apical Na-K-2Cl cotransporter of macula densa cells. *Am J Physiol Renal Physiol* 275: F703–F709, 1998.
30. **Lewis A, Di Ciano C, Rotstein OD, and Kapus A.** Osmotic stress activates Rac and Cdc42 in neutrophils: role in the hypertonicity-induced actin polymerization. *Am J Physiol Cell Physiol* 282: C271–C279, 2002.
31. **Liedtke CM and Cole TS.** Activation of NKCC1 by hyperosmotic stress in human tracheal epithelial cells involves PKC-δ and ERK. *Biochim Biophys Acta* 1589: 77–88, 2002.

Downloaded from journals.physiology.org/journal/ajpcell (106.051.226.007) on August 4, 2022.

32. **Liedtke CM, Hubbard M, and Wang X.** Stability of actin cytoskeleton and PKC-δ binding to actin regulate NKCC1 function in airway epithelial cells. *Am J Physiol Cell Physiol* 284: C487–C496, 2003.
33. **Limouze J, Straight AF, Mitchison T, and Sellers JR.** Specificity of blebbistatin, an inhibitor of myosin II. *J Muscle Res Cell Motil* 25: 337–341, 2004.
34. **Lionetto MG, Pedersen SF, Hoffmann EK, Giordano ME, and Schettino T.** Roles of the cytoskeleton and of protein phosphorylation events in the osmotic stress response in EEL intestinal epithelium. *Cell Physiol Biochem* 12: 163–178, 2002.
35. **Lytle C.** Activation of the avian erythrocyte Na-K-Cl cotransport protein by cell shrinkage, cAMP, fluoride, and calyculin-A involves phosphorylation at common sites. *J Biol Chem* 272: 15069–15077, 1997.
36. **Lytle C.** A volume-sensitive protein kinase regulates the Na-K-2Cl cotransporter in duck red blood cells. *Am J Physiol Cell Physiol* 274: C1002–C1010, 1998.
37. **Lytle C and Forbush B III.** Regulatory phosphorylation of the secretory Na-K-Cl cotransporter: modulation by cytoplasmic Cl. *Am J Physiol Cell Physiol* 270: C437–C448, 1996.
38. **Lytle C and McManus T.** Coordinate modulation of Na-K-2Cl cotransport and K-Cl cotransport by cell volume and chloride. *Am J Physiol Cell Physiol* 283: C1422–C1431, 2002.
39. **Masszi A, Di Ciano C, Sirokmány G, Arthur WT, Rotstein OD, Wang J, McCulloch CAG, Rosivall L, Mucsi I, and Kapus A.** Central role for Rho in TGF-β_1-induced α-smooth muscle actin expression during epithelial-mesenchymal transition. *Am J Physiol Renal Physiol* 284: F911–F924, 2003.
40. **Matthews JB, Smith JA, Mun EC, and Sicklick JK.** Osmotic regulation of intestinal epithelial Na^+-K^+-Cl^- cotransport: role of Cl^- and F-actin. *Am J Physiol Cell Physiol* 274: C697–C706, 1998.
41. **Matthews JB, Smith JA, Tally KJ, Awtrey CS, Nguyen H, Rich J, and Madara JL.** Na-K-2Cl cotransport in intestinal epithelial cells: influence of chloride efflux and F-actin on regulation of cotransporter activity and bumetanide binding. *J Biol Chem* 269: 15703–15709, 1994.
42. **Nakanishi S, Yamada K, Kase H, Nakamura S, and Nonomura Y.** K-252a, a novel microbial product, inhibits smooth muscle myosin light chain kinase. *J Biol Chem* 263: 6215–6219, 1988.
43. **O'Donnell ME, Martinez A, and Sun D.** Endothelial Na-K-Cl cotransport regulation by tonicity and hormones: phosphorylation of cotransport protein. *Am J Physiol Cell Physiol* 269: C1513–C1523, 1995.
44. **Pewitt EB, Hedge RS, and Palfrey HC.** [^{3}H]bumetanide binding to avian erythrocyte membranes: correlation with activation and deactivation of Na/K/2Cl cotransport. *J Biol Chem* 265: 14364–14370, 1990.
45. **Piechotta K, Garbarini N, England R, and Delpire E.** Characterization of the interaction of the stress kinase SPAK with the Na^+-K^+-$2Cl^-$ cotransporter in the nervous system: evidence for a scaffolding role of the kinase. *J Biol Chem* 278: 52848–52856, 2003.
46. **Piechotta K, Lu J, and Delpire E.** Cation chloride cotransporters interact with the stress-related kinases Ste20-related proline-alanine-rich kinase (SPAK) and oxidative stress response 1 (OSR1). *J Biol Chem* 277: 50812–50819, 2002.
47. **Plata C, Meade P, Vázquez N, Hebert SC, and Gamba G.** Functional properties of the apical Na^+-K^+-$2Cl^-$ cotransporter isoforms. *J Biol Chem* 277: 11004–11012, 2002.
48. **Russell JM.** Sodium-potassium-chloride cotransport. *Physiol Rev* 80: 211–276, 2000.
49. **Saitoh M, Ishikawa T, Matsushima S, Naka M, and Hidaka H.** Selective inhibition of catalytic activity of smooth muscle myosin light chain kinase. *J Biol Chem* 262: 7796–7801, 1987.
50. **Shen MR, Furla P, Chou CY, and Ellory JC.** Myosin light chain kinase modulates hypotonicity-induced Ca^{2+} entry and Cl^- channel activity in human cervical cancer cells. *Pflügers Arch* 444: 276–285, 2002.
51. **Shrode LD, Klein JD, Douglas PB, O'Neill WC, and Putnam RW.** Shrinkage-induced activation of Na^+/H^+ exchange: role of cell density and myosin light chain phosphorylation. *Am J Physiol Cell Physiol* 272: C1968–C1979, 1997.
52. **Straight AF, Cheung A, Limouze J, Chen I, Westwood NJ, Sellers JR, and Mitchison TJ.** Dissecting temporal and spatial control of cytokinesis with a myosin II inhibitor. *Science* 299: 1743–1747, 2003.
53. **Takeda M, Homma T, Breyer MD, Horiba N, Hoover RL, Kawamoto S, Ichikawa I, and Kon V.** Volume and agonist-induced regulation of myosin light-chain phosphorylation in glomerular mesangial cells. *Am J Physiol Renal Fluid Electrolyte Physiol* 264: F421–F426, 1993.
54. **Ye LH, Kishi H, Nakamura A, Okagaki T, Tanaka T, Oiwa K, and Kohama K.** Myosin light-chain kinase of smooth muscle stimulates myosin ATPase activity without phosphorylating myosin light chain. *Proc Natl Acad Sci USA* 96: 6666–6671, 1999.
55. **Zhao H, Hyde R, and Hundal HS.** Signalling mechanisms underlying the rapid and additive stimulation of NKCC activity by insulin and hypertonicity in rat L6 skeletal muscle cells. *J Physiol* 560: 123–136, 2004.

Downloaded from journals.physiology.org/journal/ajpcell (106.051.226.007) on August 4, 2022.